Microporous and Mesoporous Materials 174 (2013) 74–80

Contents lists available at SciVerse ScienceDirect

Microporous and Mesoporous Materials

journal homepage: www.elsevier.com/locate/micromeso

Application of the piperazine-grafted CuBTTri metal-organic framework in postcombustion carbon dioxide capture

Anita Das [a], Mohammad Choucair [a], Peter D. Southon [a], Jarad A. Mason [b], Ming Zhao [c], Cameron J. Kepert [a], Andrew T. Harris [c], Deanna M. D'Alessandro [a,*]

[a] School of Chemistry, The University of Sydney, New South Wales 2006, Australia
[b] Department of Chemistry, University of California, Berkeley, CA 94720, USA
[c] School of Chemical and Biomolecular Engineering, The University of Sydney, New South Wales 2006, Australia

ARTICLE INFO

Article history:
Received 22 November 2012
Received in revised form 22 February 2013
Accepted 23 February 2013
Available online 6 March 2013

Keywords:
Carbon dioxide capture
Piperazine
Grafted framework
Metal-organic framework

ABSTRACT

Post-synthetic modification of $H_3[(Cu_4Cl)_3(BTTri)_8]$ or CuBTTri, where H_3BTTri = 1,3,5-tris(1*H*-1,2,3-triazol-5-yl)benzene, with piperazine (*pip*) has yielded the grafted framework $H_3[(Cu_4Cl)_3(BTTri)_8(pip)_{12}]$, *pip*-CuBTTri, which exhibits an improved CO_2 uptake at pressures pertinent to postcombustion flue gas capture compared with the non-grafted material. In particular, the volumetric capacity of *pip*-CuBTTri was 2.5 times higher than that of CuBTTri at *ca.* 0.15 bar and 293 K. A chemisorption mechanism for CO_2 adsorption was proposed on the basis of diffuse reflectance infrared spectra (DRIFTS) and the high initial isosteric heat of adsorption ($-Q_{st}$, ≈96.5 kJ/mol). Application of the Ideal Adsorbed Solution Theory (IAST) to a simulated mixture of 0.15 bar CO_2/0.75 bar N_2 revealed a selectivity factor of 130. Both pressure and temperature swing processes were found to be suitable for facile regeneration of the material over multiple adsorption–desorption cycles.

1. Introduction

Methods currently implemented for CO_2 separation and capture from flue gas streams are centered on the use of aqueous solutions of primary and secondary amines ("scrubbers") that undergo a chemical reaction with CO_2 to form a carbamate [1]. The energetic costs of regenerating scrubber solutions are unsustainable; the high heat of absorption, the inherent stability of the carbamate species formed from the reaction, and the large amount of energy required to regenerate the solutions (which typically require heating to 100–140 °C) are the primary contributing factors to such inefficiencies. For example, monoethanolamine increases the energy cost of a power plant by 25–40% [2].

Sterically-hindered secondary amines are an alternative to traditional solvent systems used for CO_2 capture from coal-fired power plants. They possess both a rapid rate of reaction compared with the primary and secondary amines currently used in industry, as well as a lower heat of reaction and reduced carbamate stability. These factors compromise between selectivity for CO_2, total CO_2 uptake, and the regeneration of the sorbent used. Piperazine is an example of one such amine, having a high rate of reaction with CO_2 and effectively promoting the removal of CO_2 from flue gas streams [3]. Furthermore, the addition of piperazine to aqueous potassium carbonate solutions has been shown to increase the heat of absorption of CO_2 from 15 to 42 kJ/mol, [4] indicating that it may be useful in modulating the strength of interaction between CO_2 and absorbents which would otherwise have a relatively low affinity for the gas.

Despite the advantages of using piperazine over other amine solvents, the corrosive nature of these solutions remains problematic. Due to this inherent drawback, they are typically used as 25–30 wt.% aqueous mixtures, of which the water content (with its high heat capacity) contributes a significant energy cost to heating and regenerating the solvent in conventional 'wet scrubbing' processes. Such issues leading to the inefficient demands for energy consumption underpin the shift from solution-state solvents to solid-state materials.

The application of novel adsorbents in postcombustion schemes requires that these materials possess a high selectivity and capacity for CO_2, stability to extreme industrial conditions, and a low energy cost for regeneration [5,6]. Metal-organic frameworks (MOFs) are a prospective class of materials for industrial application due to their high surface areas and porosities, as well as their tunable structural and chemical features. The history and successes of MOFs for carbon dioxide capture have been documented recently in several excellent reviews [7–10]. Despite these successes, many MOFs are incompatible with flue stream conditions either by virtue of their low selectivity for carbon dioxide over other components in flue gas (particularly N_2 and H_2O) or their low uptakes in the 0.1–0.15 bar pressure region (the partial pressure of CO_2 in flue gas).

* Corresponding author. Tel.: +61 (2) 9351 3777; fax: +61 (2) 9351 3329.
E-mail address: deanna@chem.usyd.edu.au (D.M. D'Alessandro).

1387-1811/$ - see front matter © 2013 Elsevier Inc. All rights reserved.
http://dx.doi.org/10.1016/j.micromeso.2013.02.036

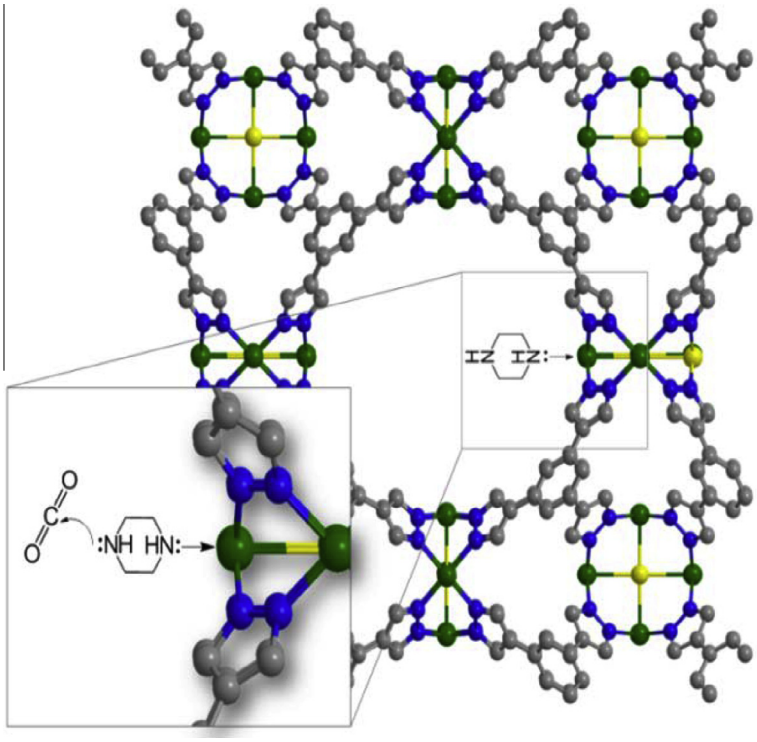

Fig. 1. Schematic representation of the appended framework, *pip*-CuBTTri. The magnified region shows the grafting of *pip* to CuBTTri, and the chemical affinity of the 'free' N-H for CO_2.

It has been shown that the adsorption capacity and selectivity of MOFs for CO_2 over other components in a flue stream can be maximised by introducing polarising groups (*e.g.* alkylamine [11] or fluoro [12] moieties, coordinated water molecules [13]) into the pore space to selectively interact with carbon dioxide. Several established techniques now exist for the implementation of post-synthetic modifications without impacting the MOF scaffold, including the exploitation of non-covalent interactions (host–guest exchange), covalent interactions (post-synthetic modifications of the organic linker component of the MOF), and coordinative interactions (metal–ligand interactions) [14]. Specifically, coordinative interactions enable the introduction of ligands into the framework without altering its structure; if introduced during MOF synthesis, such ligands may interfere with or prevent the formation of the material.

By analogy with liquid alkanolamine absorbents traditionally used for postcombustion capture, similar amine-based moieties have been incorporated into MOFs through coordinative interactions with open metal sites to enhance CO_2 selectivity [15]. Although this comes at the expense of reducing the available surface area, it is envisioned that the selectivity and overall capacity for CO_2 may be optimised in these "grafted" MOFs. This approach has been employed previously with ethylenediamine (*en*), [15] *N*-methylethylenediamine (*men*) and *N,N′*-dimethylethylenediamine (*mmen*) [16] in the CuBTTri framework; *en* in the Mg_2(dobdc) framework [17] and *mmen* in the Mg_2(dobpdc) framework [18] (dobdc = 1,4-dioxido-2,5-benzenedicarboxylate; dobpdc = 4,4-dioxido-3,3-biphenyldicarboxylate). The compounds *mmen*-CuBTTri and *mmen*-Mg_2(dobpdc) exhibit some of the highest selectivities and binding strengths for CO_2 over N_2 at 0.1–0.15 bar compared to any MOF reported to date, highlighting the utility of secondary amines in improving the selectivity of known materials for CO_2 capture [16,18].

Inspired by current interest in the industrial application of piperazine in postcombustion chemical absorption processes, and recent results demonstrating the enhanced selectivity of piperazine-grafted Ni_2(dobdc) for CO_2 over N_2 [19], we investigate the application of *pip*-CuBTTri (where CuBTTri = $H_3[(Cu_4Cl)_3(BTTri)_8]$) for stationary postcombustion CO_2 capture (with pressure and temperature swing-based regeneration). The CuBTTri framework is known to exhibit high air, water, and thermal stability, and has been studied extensively for carbon dioxide capture due to its high capacity for CO_2 at room temperature and at the low partial pressures pertinent in postcombustion flue gas separation [20]. Although similar works on amine grafted MOFs for CO_2 capture have appeared, including the authors' previous reports [16,19], this work explores the influence of the piperazine function. In particular, we provide a detailed analysis and discussion based on the comparison with related amine-grafted CuBTTri frameworks (*mmen*-CuBTTri), which proves helpful in understanding the adsorption of CO_2 in amine-grafted MOFs.

The grafted material can be generated via the post-synthetic introduction of the secondary amine, *pip*, to yield *pip*-CuBTTri (Fig. 1). The possible mechanisms driving CO_2 uptake, and the framework stability during regenerative pressure and temperature swing cycles are investigated. Of particular interest is how subtle changes in the steric properties of alkylamines influence the CO_2 uptake and selectivity of CuBTTri.

2. Experimental section

2.1. Synthesis

2.1.1. Synthesis of CuBTTri

CuBTTri was synthesised according to literature procedures [15]. Powder X-ray diffraction (PXRD) confirmed the identity of the product formed, and the pattern was identical to that reported previously. The resulting powder was washed with methanol via Soxhlet extraction for 24 h and activated at 180 °C under vacuum.

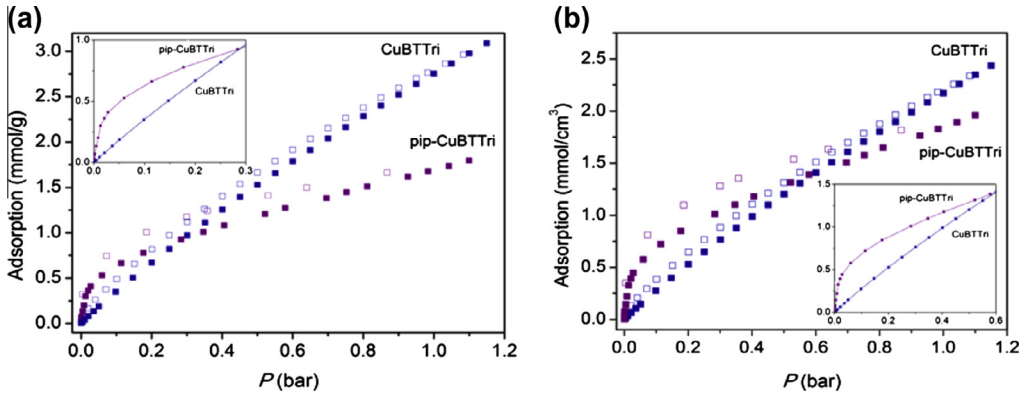

Fig. 2. Gravimetric (a) and volumetric (b) isotherms for CO_2 adsorption (closed symbols) and desorption (open symbols) at 293 K in CuBTTri and *pip*-CuBTTri. Insets in each figure are shown to highlight the improvement in low pressure CO_2 uptake in the appended material. Lines are given to guide the eye.

2.1.2. Post-synthetic modification of CuBTTri with piperazine, $H_3[(Cu_4Cl)_3(BTTri)_8(C_4H_{10}N_2)_{12}]\cdot 8H_2O$, (pip-CuBTTri)

Under a nitrogen atmosphere, fully activated CuBTTri (81 mg) was suspended in freshly distilled diethyl ether and piperazine ($C_4H_{10}N_2$, 60 mg, 2.3 eq. per unsaturated Cu^{II} site) was added with stirring. The initially red–brown compound immediately attained a green–blue colouration and the suspension was stirred at room temperature for a further 72 h. The solid was collected by vacuum filtration and washed copiously with successive aliquots of diethyl ether (5×5 mL) to remove unreacted piperazine. The solid was then dried at 50 °C under reduced pressure to remove excess solvent. PXRD was used to confirm the crystallinity of the product. Anal. Calcd. for $C_{144}H_{188}Cl_3Cu_{12}N_{96}O_8$ (MW = 4260.6 g/mol): C 41.91, H 4.89, N 29.21. Found: C 40.59, H 4.45, N 31.56. Powder X-ray diffraction data showed this framework to be isostructural to $H[Cu(DMF)_6][(Cu_4Cl)_3(BTT)_8(H_2O)_{12}]\cdot 3.5HCl\cdot 12H_2O\cdot 16CH_3OH$ (CuBTT where H_3BTT = 1,3,5-tris(tetrazol-5-yl)benzene) [21] with a Le Bail refinement using the observed peak positions revealing a cubic unit cell parameter of a = 18.724 Å.

2.2. Characterization

2.2.1. Gas adsorption measurements

Adsorption isotherms were measured using the Accelerated Surface Area & Porosimetry System (ASAP) 2020 supplied by Micromeritics Instruments Inc. Approximately 100 mg of sample was loaded into a glass analysis tube and outgassed for 12 h under vacuum at 80 °C prior to measurement. N_2 adsorption and desorption isotherms were measured at 77 K and data were analysed using a Brunauer–Emmett–Teller (BET) model to determine the surface area [22]. CO_2 measurements (up to 1 bar) were carried out on the ASAP2020 as described above. The heat of adsorption for CO_2 was determined by comparing isotherms at 293, 303 and 313 K. Isosteric heat of adsorption calculations ($-Q_{st}$)[1] for CO_2 at these temperatures were undertaken using the Clausius–Clapeyron equation using the interpolation function in OriginPro 8 to fit the isotherms [15].

2.2.2. Selectivity factor determinations

The single component selectivity factor for adsorption of CO_2 over N_2 in *pip*-CuBTTri was estimated from the single-component N_2 and CO_2 room temperature isotherm data. The values for this approximation are derived from an approximate flue gas composition of 15% CO_2, 75% N_2, and 10% other gases, at a total pressure of 1 bar. Hence, the value is normalised for the pressures of CO_2 at 0.15 bar to the adsorbed amount of N_2 at 0.75 bar, according to Eq. (1), where n is the quantity of gas adsorbed in mmol/g and x is the equilibrium partial pressure (P) in bar at which each gas is adsorbed.

$$S = \frac{n\mathrm{CO_2}/n\mathrm{N_2}}{x\mathrm{CO_2}/x\mathrm{N_2}} \tag{1}$$

The Ideal Adsorbed Solution Theory (IAST) was employed to model the mixed gas behavior in a binary CO_2/N_2 mixture from the experimentally measured single component isotherms [23]. In order to apply IAST, it was first necessary to mathematically fit the single component CO_2 and N_2 adsorption isotherms. In both cases, a Langmuir model was used for this purpose. For N_2 adsorption in *pip*-CuBTTri at 293 K, a single-site Langmuir equation was used (Eq. (2)), where n is the amount adsorbed in mmol/g, q_{sat} is the saturation capacity in mmol/g, b is the Langmuir parameter in bar^{-1}, and P is the pressure in bar. Note that IAST calculations are extremely sensitive to the saturation capacity of the most weakly adsorbing component. Without high-pressure adsorption data, it is important to accurately fit the saturation capacity in order to obtain a meaningful IAST result. In a previous study, the q_{sat} for room temperature N_2 adsorption in *mmen*-CuBTTri was found to be 5 mmol/g [16]. By accounting for the reduced surface area of *pip*-CuBTTri, the N_2 saturation capacity was estimated based on this value.

$$n = \frac{q_{sat}bP}{1+bP} \tag{2}$$

For CO_2 adsorption in *pip*-CuBTTri at 293 K, a dual-site Langmuir Freundlich equation was used (Eq. (3)), where n is the amount adsorbed in mmol/g, P is the pressure in bar, $q_{sat,i}$ is the saturation capacity in mmol/g, b_i is the Langmuir parameter in bar^{-1}, and v_i is the Freundlich parameter for two sites a and b.

$$n = \frac{q_{sat,a}b_aP^{v_a}}{1+b_aP^{v}} + \frac{q_{sat,b}b_bP^{v_b}}{1+b_bP^{v}} \tag{3}$$

A CO_2/N_2 selectivity factor, S, can then be calculated using Eq. (1), where n is the amount of each component adsorbed as determined from IAST and x is the mole fraction of each component in the gas phase at equilibrium.

2.2.3. Thermogravimetric analysis and gas cycling measurements

Thermogravimetric Analysis cycling experiments were carried out on a TA Instruments TGA Q5000IR using alternating flows of CO_2 (4 mL/min) with N_2 (21 mL/min) and pure N_2 (25 mL/min).

[1] $-Q_{st}$ is quoted as a positive value for ease of comparison with data commonly reported the literature. It is noted, however, that from a thermodynamic point of view, the values derived from such adsorbate-adsorbent interactions are strictly negative (exothermic).

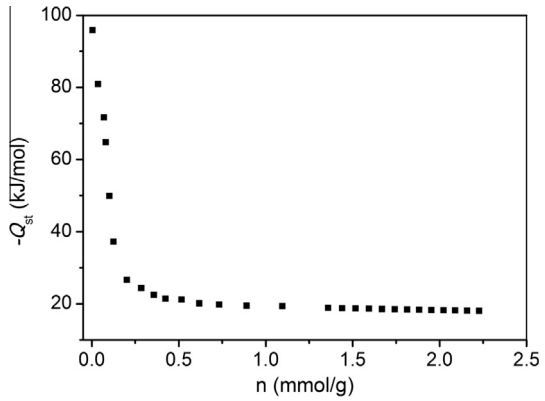

Fig. 3. Isosteric heats of adsorption for CO_2 in *pip*-CuBTTri obtained from fits to the gas adsorption data collected at 293, 303 and 313 K. Isosteric heat of adsorption calculations ($-Q_{st}$) for CO_2 at these temperatures were undertaken using the Clausius–Clapeyron equation using the interpolation function in OriginPro 8 to fit the isotherms.[13]

Prior to cycling, the sample was activated by heating at 80 °C for 90 min, followed by cooling to 40 °C under a N_2 atmosphere. The sample mass was normalised to 0% at 40 °C under a nitrogen atmosphere and is uncorrected for buoyancy effects.

The adsorption and desorption of CO_2 during two sets of temperature swing cycles (25–50 °C and 25–80 °C) was measured using a Hiden-Isochema IGA-002 gravimetric system. The sample was activated under high vacuum ($<10^{-5}$ mbar) at the maximum temperature to be used in the measurement cycle. The sample was then cooled to 25 °C and dosed with 0.150 bar of CO_2. Once the equilibrium mass was attained, the sample temperature was cycled between 25 °C and either 50 or 80 °C, while the CO_2 pressure was maintained at 0.150(4) bar. Each 50 °C cycle was conducted over 2 h and each 80 °C cycle over 3 h.

2.2.4. Infrared and DRIFTS measurements

In situ diffuse reflectance infrared Fourier transform spectroscopy (DRIFTS) was performed on samples in a potassium bromide matrix over the range 4000–400 cm^{-1} using a Praying Mantis (Harrick Scientific Products, Inc.) attachment on a Tensor 27 (Bruker) FT-IR spectrometer. The Praying Mantis was mounted with a Low Temperature Reaction Chamber fitted with ZnSe windows and Temperature Controller (Harrick Scientific Products, Inc.). The sample was heated at 80 °C under vacuum for 16 h prior to analysis. High purity CO_2 (99.99%) was introduced at a range of pressures, and 1600 scans of the sample were recorded and averaged at each pressure dose.

2.2.5. Other physical measurements

PXRD data were collected over the 5–50° 2θ range with a 0.02° step size and 2°/min scan rate on a PANalytical X′Pert Pro diffractometer fitted with a solid-state PIXcel detector (40 kV, 30 mA, 1° divergence and anti-scatter slits, and 0.3 mm receiver and detector slits) using Cu-K_α (λ = 1.5406 Å) radiation. Elemental analyses were conducted at the Campbell Microanalytical Laboratory, University of Otago, New Zealand. Samples were dried by heating under vacuum immediately prior to analysis.

3. Results and discussion

The grafting reaction of CuBTTri with piperazine resulted in a marked colour change in the framework from red–brown to green–blue. PXRD data indicated that the structure of the framework was unchanged from that of the bare material (Fig. S1), with a similar unit cell parameter of a = 18.724 Å. Elemental analysis results were consistent with a formula of $H_3[(Cu_4Cl)_3(BTTri)_8(C_4H_{10}N_2)_{12}].8H_2O$ which corresponds to one piperazine molecule per Cu^{II} site.

Nitrogen adsorption and desorption isotherms were carried out at 77 K on both the appended and bare frameworks (see SI, Fig. S2). Both isotherms exhibit Type I behaviour (as defined by IUPAC) [24] which is indicative of a microporous material. This is supported by the calculated BET surface areas for CuBTTri and *pip*-CuBTTri of 1700 m^2/g (1340 m^2/cm^3) [15] and 380 ± 1 m^2/g (415 m^2/cm^3), respectively. Compared with the parent material, the appended framework possesses 30% of the surface area by volume, but only 20% by weight. Additionally, the appended framework tends towards N_2 saturation at a lower rate than the appended framework, as expected due to the restricted pore volume which results in a decreased accessibility to guest molecules (Fig. S3). Previously synthesised amine-appended MOFs were also characterised by reduced surface areas, consistent with our results [15,16,18]. In the present case, the surface area of *pip*-CuBTTri is similar to that of *en*-CuBTTri (BET surface area 345 m^2/g)[12] containing the primary amine ethylenediamine; however, both frameworks are sufficiently porous to be considered as candidates for gas separation [7].

The appended framework, *pip*-CuBTTri, showed an improved CO_2 uptake at the low pressures pertinent to postcombustion capture from flue gas when compared to the bare framework (0.75 mmol/g in *pip*-CuBTTri compared to 0.50 mmol/g in CuBTTri at *ca.* 0.15 bar) (Fig. 2). The slight hysteresis observed in the sorption isotherm for the appended framework is suggestive of its improved affinity for CO_2; however, the overall CO_2 uptake at 1 bar was reduced due to the decreased porosity (1.8 mmol/g compared to 3.1 mmol/g in CuBTTri) (Fig. 2a). Interestingly, the reduction in the CO_2 uptake at 1 bar is not directly proportional to the decrease in surface area: a 74% reduction in surface area is observed compared with only a 40% reduction in the CO_2 uptake. The amount of CO_2 adsorbed in the appended material is higher relative to the amount that would be expected based on the diminished surface area, suggesting that the addition of polarising amine sites in *pip*-CuBTTri has a positive impact on CO_2 adsorption even in light of the inevitable reduction of surface area.

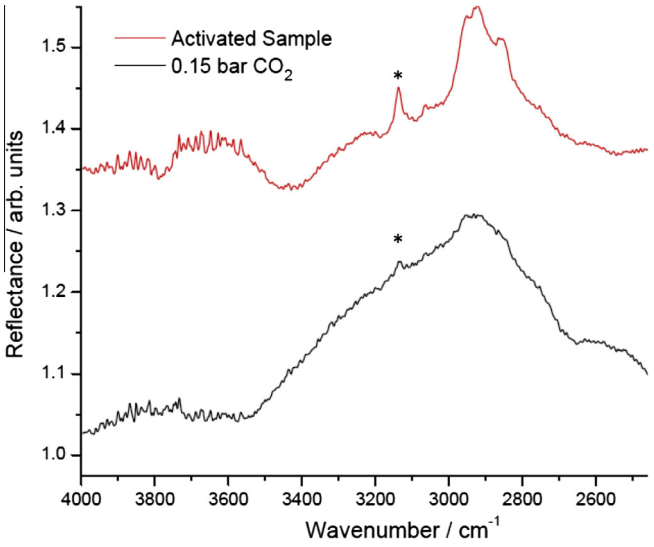

Fig. 4. DRIFTS spectra of CO_2 adsorption in *pip*-CuBTTri. The disappearance of the band at *ca.* 3150 cm^{-1} is a strong indication that CO_2 adsorption occurs *via* a chemical adsorption mechanism.

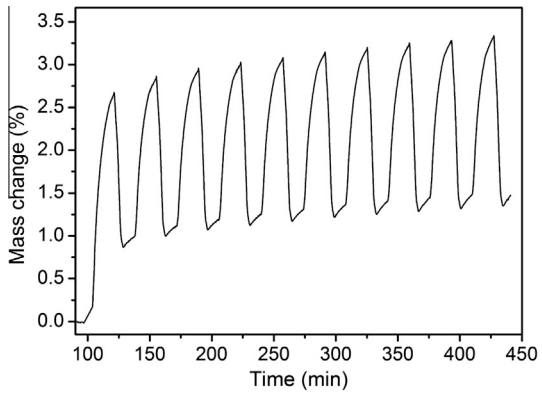

Fig. 5. TGA cycling experiment on *pip*-CuBTTri employing alternating flows of CO_2 (4 mL/min) in N_2 (21 mL/min) and pure N_2 (25 mL/min) over 10 cycles at 40 °C.

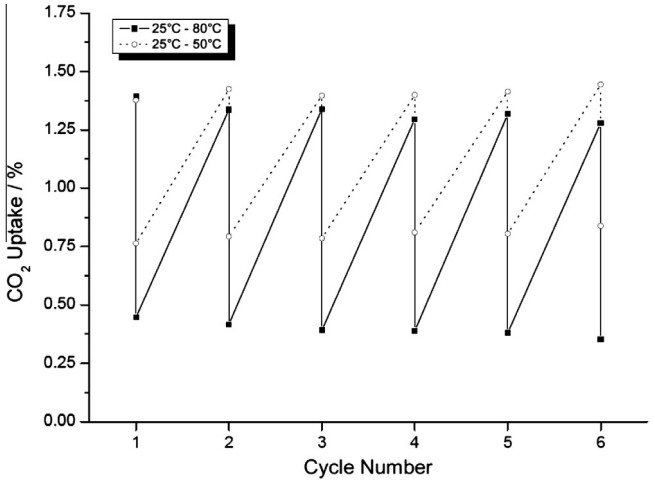

Fig. 6. Temperature cycling experiment performed on *pip*-CuBTTri at 0.15 bar CO_2. The points collected measure the total CO_2 uptake and read vertically along each cycle number, with the lines joining successive points of each cycle indicating the start and end. Experiments were performed at 25–50 °C and 25–80 °C.

For stationary applications such as postcombustion CO_2 capture, the volumetric capacity, which takes into account the density of the material and crystallite packing, is often a better indicator of performance than gravimetric capacity. This is due to the industrial importance of the volume that the adsorbent occupies, rather than its weight. Fig. 2 shows the gravimetric and volumetric gas adsorption isotherms for CuBTTri and *pip*-CuBTTri. While a 38% increase in the framework density occurs upon grafting with *pip,* there is no significant change in the volume, such that the volumetric capacity of *pip*-CuBTTri is significantly improved compared with the gravimetric capacity. For example, at 1 bar there is a 20% reduction in CO_2 uptake according to the volumetric capacity, compared to a 40% reduction in the gravimetric CO_2 uptake of *pip*-CuBTTri versus CuBTTri. Incidentally, the molar (Fig. S4) and volumetric capacities of the framework exhibit similar profiles, indicating that *ca.* 80% of the capacity is retained per binding site.

The polarising amine sites in *pip*-CuBTTri appear to selectively enhance CO_2 sorption over N_2 sorption in the appended framework with a calculated single component selectivity factor of 20 at 0.15 bar CO_2/0.75 bar N_2 (based on gravimetric adsorption data). While the single-component calculation provides an estimate of selectivity between the two gases, a more comprehensive adsorption model such as Ideal Adsorbed Solution Theory (IAST) can be employed to more accurately predict mixed gas behaviour in binary mixtures from experimentally measured single component isotherms [23]. The accuracy of the IAST procedure has already been established for a wide variety of gas mixtures in different zeolites, [25] and for CO_2 capture within MOFs [26,27]. Here, IAST is used to provide an estimate of the selectivity of *pip*-CuBTTri for CO_2 over N_2 under conditions representative of a dry flue gas. The IAST CO_2/N_2 selectivity factor of *pip*-CuBTTri for a gas mixture containing 0.15 bar CO_2 and 0.75 bar N_2 at 293 K is 130, which is significantly lower than the value of 327 for *mmen*-CuBTTri [16]. Thus, despite the comparable extents of grafting in *pip*-CuBTTri and *mmen*-CuBTTri (both contain approximately one amine per Cu^{II} site), it would appear that the introduction of a comparatively less sterically-hindered secondary amine does not increase the selectivity of CO_2/N_2 separation.

The isosteric heat of adsorption ($-Q_{st}$) data shown in Fig. 3 indicate that *pip*-CuBTTri exhibits a strong initial interaction with CO_2 as binding occurs to the 'free' amine sites, as evidenced by a large $-Q_{st}$ of 96.5 kJ/mol at approximately zero coverage. The high heat of adsorption and specific affinity for CO_2 over N_2 are indicative of a chemical adsorption process, which is likely to involve an interaction between the relatively electrophilic carbon atom of CO_2 and the lone pair of the 'free' amine of piperazine (Fig. 1). The isosteric heat of adsorption decreases rapidly to *ca.* 20 kJ/mol with loading beyond n = 0.25 mmol/g, indicating that the number of amines that strongly adsorb CO_2 is considerably less than the number of *pip* in the framework. Thus, despite the improved CO_2 uptake and selectivity at 0.15 bar compared with the bare framework, this is not borne out by the magnitude of $-Q_{st}$ which is approximately the same for the two frameworks at this pressure. The point of inflection in the heat of adsorption profile appears to differentiate pressures at which CO_2 is chemisorbed into the framework (*i.e.* bound to the amine sites) compared to pressures at which it is physisorbed [15,16]; this inflection occurs at n = 0.25 mmol/g, indicating that only 10% of the total number of 'free' amine sites are bound by CO_2. It is feasible that the initial chemisorption interaction between CO_2 and the amine sites facilitates subsequent CO_2 physisorption into the framework, as well as co-adsorption of CO_2 molecules *i.e.*, host–guest interactions which facilitate guest–guest interactions.

A comparison between the isosteric heat of adsorption profiles for *pip*-CuBTTri and the closely-related *mmen*-CuBTTri [16] framework (also containing approximately one amine per Cu^{II} site) reveals a comparable initial isosteric heat of adsorption, followed by a more rapid decrease in $-Q_{st}$ with increasing n in the former case. Notwithstanding the smaller surface area for *pip*-CuBTTri (380 *vs* 870 m^2/g for *mmen*-CuBTTri [16]), the more sterically-accessible nature of the 'free' N-H amine of *pip* compared with the more sterically-encumbered *mmen* does not lead to the expected increase in $-Q_{st}$ at 0.15 bar (corresponding to n ≈2.4 mmol/g).

Previous literature reports for *en*-CuBTTri revealed a similar rapid decline in the isosteric heat of adsorption with loading which was ascribed to the fact that not all *en* are bound to open metal sites [15,16]. Excess amines may lead to pore blockage which decreases the surface area and reduces the accessibility of otherwise 'free' N-H sites to guest CO_2 molecules. A similar explanation may be reasonable in the present case, indicating that reducing the degree of steric hindrance in a secondary amine does not necessarily lead to the anticipated improvement in the CO_2 uptake and selectivity: when the more sterically-encumbered secondary amine *mmen* was incorporated into CuBTTri, the grafted material exhibited a higher surface area and superior CO_2 selectivity compared with *pip*-CuBTTri. By comparison, in aqueous solutions, steric hindrance and basicity are known to control reactions between CO_2 and amines [28]. In amine-grafted frameworks under dry CO_2/N_2 conditions, it is evident that a more complicated set of competing

factors control reactions between CO_2 and amines, rendering steric predictions impossible. Clearly, understanding the influence of water vapour on the CO_2 capture process in framework materials represents an important goal of future work.

In situ DRIFTS measurements were carried out to confirm the primary nature of the CO_2-amine interaction within the framework (Fig. 4). At 298 K, 0.15 bar of ultrapure CO_2 was introduced into the vacuum tight chamber containing a sample of activated *pip*-CuBTTri. A prominent decrease in intensity of the N-H band at *ca.* 3150 cm^{-1} was observed which was followed by the reappearance of this band upon regeneration of the material under heat (80°C) and vacuum. This behaviour strongly supports the proposed chemisorption interaction between CO_2 and the 'free' amine site of piperazine. It must be noted that previous spectroscopic studies of CO_2 capture in amine-appended MOFs such as amine-functionalised MIL-53 (Al(OH)[O_2C–$C_6H_3NH_2$–CO_2]) have illustrated that CO_2 sorption may not be caused by a direct arylamine-CO_2 interaction, but instead by other physisorptive processes [29]. In the present case, the high initial isosteric heat of adsorption in *pip*-CuBTTri in addition to the spectroscopic evidence strongly supports a primary chemical adsorption mechanism for the alkylamine-CO_2 interaction.

The regenerative capacity of the framework using a pressure swing adsorption process was probed using TGA cycling experiments at 40 °C over 10 cycles, initially with no temperature swing (Fig. 5). Following activation of the material, a flow of CO_2 (4 mL/min, *ca.* 0.15 bar partial pressure) was introduced into the furnace for 30 min leading to an increase in the sample mass by *ca.* 2.6%. The material was subsequently regenerated with a pure N_2 purge for 30 min, resulting in a decrease in the sample mass of *ca.* 1.8% to a value approaching the original sample mass measured prior to the introduction of CO_2. Interestingly, the incomplete regeneration of the material following the first cycle of *ca.* 0.9 wt.% (0.2 mmol/g) is approximately equivalent to the number of chemisorbed piperazine sites according to the calculated isosteric heat of adsorption (Fig. 3), suggesting that these sites may require slightly more forcing conditions to be regenerated. Aside from the incomplete regeneration of the material in the first cycle, there was no significant loss in capacity after 9 cycles.

The regenerative capacity of *pip*-CuBTTri was further investigated using a temperature swing adsorption process in the region of 0.15 bar partial pressure of CO_2 by loading an activated sample with CO_2 and swinging the temperatures between 25–50 °C and 25–80 °C (Fig. 6). Regeneration of the sample between 25 °C and 80 °C resulted in the removal of more than 66% of adsorbed CO_2 in *pip*-CuBTTri. This adsorption–desorption process was performed consistently with no significant loss over 6 cycles. Likewise, the temperature swings up to 50 °C resulted in the removal of almost 50% of the adsorbed CO_2, significantly lowering the amount of energy required for regeneration per cycle.

4. Conclusions

Inspired by current interest in the use of piperazine as an additive to improve the absorption properties of aqueous alkanolamine solutions for postcombustion 'wet scrubbing', the CO_2 uptake and selectivity of the piperazine-grafted CuBTTri framework were investigated. Despite the reduced surface area of *pip*-CuBTTri relative to the non-grafted framework and the apparently low availability of accessible 'free' secondary amines of *pip* for CO_2 chemisorption, the dominance of these sites on the low pressure behaviour endows the grafted material with an improved CO_2 uptake at pressures pertinent to postcombustion flue gas capture. Indeed, the material is remarkably well optimised for low pressure CO_2 uptake despite the rapid decrease in $-Q_{st}$. Importantly, the volumetric capacity of *pip*-CuBTTri – which is a critical consideration for stationary applications such as postcombustion capture – was 2.5 times higher than that of the non-grafted material at 0.15 bar and 293 K. The origin of the selectivity enhancement is attributable to a chemisorption interaction between CO_2 and the 'free' secondary amine of *pip*. A mild pressure or temperature swing adsorption process was found to be suitable for facile regeneration of the material over multiple adsorption–desorption cycles.

A comparison of the results for *pip*-CuBTTri with the closely related *mmen*-CuBTTri framework [15] reveals that despite the relatively more sterically-accessible nature of *pip* compared with *mmen*, this is not manifested by a corresponding improvement in the CO_2 uptake. Thus, while steric hindrance and basicity are known to control reactions between CO_2 and amines in aqueous solutions, [27] predicting the influence of sterics on adsorption properties of framework systems under dry conditions is not straightforward.

Clearly, gaining an understanding of gas adsorption in the presence of water vapour is a key to future efforts to design improved alkylamine-grafted frameworks for CO_2 capture. At the present time, it would appear that the integration of secondary amines possessing a high degree of steric hindrance (such as *mmen*) into frameworks endows these materials with superior performance characteristics. By employing post-synthetic modification procedures in frameworks with larger pore spaces, and by integrating ligands with covalently tethered alkylamines, it is likely that improved overall CO_2 uptakes could be achieved in addition to low pressure selectivity. Ultimately, the selection of an industrially-viable material will necessarily require a compromise between total uptake at 0.15 bar, selectivity for CO_2 over other components in a flue stream, and the energy cost for regeneration.

Acknowledgements

This work was supported by The University of Sydney and the Science and Industry Endowment Fund (SIEF). We gratefully acknowledge Professor Jeff Long for his encouragement throughout this project.

Appendix A. Supplementary data

Supplementary data associated with this article can be found, in the online version, at http://dx.doi.org/10.1016/j.micromeso.2013.02.036.

References

[1] P.D. Vaidya, E.Y. Kenig, Chem. Eng. Technol. 30 (2007) 1467–1474.
[2] G.T. Rochelle, Science 325 (2009) 1652–1654.
[3] S. Bishnoi, G.T. Rochelle, Chem. Eng. Sci. 55 (2000) 5531–5543.
[4] J.T. Cullinane, G.T. Rochelle, Chem. Eng. Sci. 59 (2004) 3619–3630.
[5] R.S. Haszeldine, Science 325 (2009) 1647–1652.
[6] The National Mining Association of the American Mining Industry Status of CCS Development, The National Mining Association of the American Mining Industry: Carbon Capture and Storage Technologies, http://www.nma.org/ccs/.
[7] D.M. D'Alessandro, B. Smit, J.R. Long, Angew. Chem. Int. Ed. Engl. 49 (2010) 6058–6082.
[8] J. Liu, P.K. Thallapally, B.P. McGrail, D.R. Brown, J. Liu, Chem. Soc. Rev. 41 (2012) 2308–2322.
[9] K. Sumida, D.L. Rogow, J.A. Mason, T.M. McDonald, E.D. Bloch, Z.R. Herm, T.-H. Bae, J.R. Long, Chem. Rev. 112 (2011) 724–781.
[10] J.-R. Li, Y. Ma, M.C. McCarthy, J. Sculley, J. Yu, H.-K. Jeong, P.B. Balbuena, H.-C. Zhou, Coord. Chem. Rev. 255 (2011) 1791–1823.
[11] C. Janiak, Dalton Trans. (2011) 724–781.
[12] W.W. Xu, S. Pramanik, Z. Zhang, T.J. Emge, J. Li, J. Solid State Chem. 200 (2013) 1–6.
[13] S. Xiang, Y. He, Z. Zhang, H. Wu, W. Zhou, R. Krishna, B. Chen, Nat. Commun. 3 (2012) 954.
[14] Z. Wang, S.M. Cohen, Chem. Soc. Rev. 38 (2009) 1315–1329.
[15] A. Demessence, D.M. D'Alessandro, M.L. Foo, J.R. Long, J. Am. Chem. Soc. 131 (2009) 8784–8786.

[16] T.M. McDonald, D.M. D'Alessandro, R. Krishna, J.R. Long, Chem. Sci. 2 (2011) 2022–2028.
[17] S. Choi, T. Watanabe, T.-H. Bae, D.S. Sholl, C.W. Jones, J. Phys. Chem. Lett. 3 (2012) 1136–1141.
[18] T.M. McDonald, W.R. Lee, J.A. Mason, B.M. Wiers, C.S. Hong, J.R. Long, J. Am. Chem. Soc. 134 (2012) 7056–7065.
[19] A. Das, P.D. Southon, M. Zhao, C.J. Kepert, A.T. Harris, D.M. D'Alessandro, Dalton Trans. (2012) 11739–11744.
[20] A.C. Kizzie, A.G. Wong-Foy, A.J. Matzger, Langmuir 27 (2011) 6368–6373.
[21] M. Dincă, W.S. Han, Y. Liu, A. Dailly, C.M. Brown, J.R. Long, Angew. Chem. Int. Ed. 46 (2007) 1419–1422.
[22] S. Brunauer, P.H. Emmett, E. Teller, J. Am. Chem. Soc. 60 (1938) 309–319.
[23] A.L. Myers, J.M. Prausnitz, AIChE J. 11 (1965) 121–127.
[24] K.S.W. Sing, D.H. Everett, R.A.W. Haul, L. Moscou, R.A. Pierotti, J. Rouquerol, T. Siemieniewska, in: Handbook of Heterogeneous Catalysis, Wiley-VCH Verlag GmbH & Co. KGaA, Weinheim, Germany, 2008.
[25] R. Krishna, S. Calero, B. Smit, Chem. Eng. J. 88 (2002) 81–94.
[26] R. Krishna, J.M. van Baten, Chem. Eng. J. 133 (2007) 121–131.
[27] R. Krishna, J.M. van Baten, Phys. Chem. Chem. Phys. 13 (2011) 10593–10616.
[28] G. Sartori, D.W. Savage, Ind. Eng. Chem. Fund. 22 (1983) 239–249.
[29] E. Stavitski, E.A. Pidko, S. Couck, T. Remy, E.J.M. Hensen, B.M. Weckhuysen, J. Denayer, J. Gascon, F. Kapteijn, Langmuir 27 (2011) 3970–3976.